Published by :
http://www.ijert.org

International Journal of Engineering Research & Technology (IJERT)
ISSN: 2278-0181
Vol. 13 Issue 07, July-2024

Effects of Annealing and Silar Cycles on the Structural and Optical Properties of Nio-Zno Nanocomposite Thin Films

Sandeep Kumar Soni
Department of Physics, Government V.Y.T. PG Autonomous College, Durg (C.G.), India

R. S. Singh
Department of Physics, Government V.Y.T. PG Autonomous College, Durg (C.G.), India

Pankaj Soni
Department of Chemistry, Government Danveer Tularam Postgraduate College, Utai, Distt.-Durg (C.G.),India

Abstract - Effects of annealing and SILAR cycles on the structural and optical properties of NiO-ZnO nanocomposite thin films deposited through Successive Ionic Layer Adsorption and Reaction (SILAR) technique on glass substrate were studied using X-ray diffraction (XRD), Fourier Transform-Infrared (FTIR) spectroscopy and UV-visible spectrophotometer in the range (300-800nm). Both XRD and FTIR results confirmed that annealing changed the hydroxide phase into oxide phase. Optical studies showed abrupt decrease in absorbance at the onset of visible range, absorbance increased and optical band gap values of the films decreased as the no. of SILAR cycle increased. Annealed films showed less absorbance value and less optical optical band gap value as compared to unannealed films for equal SILAR cycles.

Keyword: **NiO-ZnO, Optical band gap, Nanocomposite, XRD, SILAR.**

I. INTRODUCTION

Metal oxide nanocomposites have gained considerable popularity due to their use in an extensive range of applications such as energy storage, environmental refinements, gas sensing, ceramic production, biomedical research and catalysis [1-3]. The physical properties of the nanocomposite films are superior to those of the individual metal oxides when examined separately making these films suitable for innovative applications [4-8]. NiO-ZnO is one of the nanocomposite potentially used in solar photovoltaic [9].

Numerous methods have been commonly employed to fabricate thin films of ZnO and NiO [10-13].In this study we have deposited NiO-ZnO composites with equal 0.6M cationic precursor ratios for NiO and ZnO directly onto glass plates using the SILAR technique. SILAR is an easy and economical method for creating thin films with precise thickness and composition control. This process involves alternating the substrate's exposure to metal precursors and a reactant allowing layer-by-layer growth of the desired material [14-15]. Films have been deposited for different SILAR cycles followed by heat treatment. In this work structural and optical properties of both unannealed and annealed films have been examined.

II. EXPERIMENTAL

A. Materials

The preparation of NiO-ZnO composite thin films utilized analytical-grade zinc acetate dihydrate ($Zn(CH_3COO)_2.2H_2O$) and nickel nitrate hexahydrate ($Ni(NO_3)_2.6H_2O$) which were purchased from HiMedia Laboratories Pvt. Ltd., hydrogen peroxide solution from Loba Cheme Pvt. Ltd. and 25% aqueous ammonia (NH_4OH) from Pallav Chemicals. Distilled water was prepared in lab and flat glass substrates (75 mm x 2.5 mm x 1.3 mm) were used for film deposition.

B. Deposition of the NiO-ZnO composite thin films

The SILAR technique was used to deposit the NiO-ZnO composite thin films on glass substrate. The glass substrates were cleaned using chromic acid followed by rinsing in distilled water before deposition of films. The cationic solutions of 0.6M was prepared using $[Ni(NO_3)_2].6H_2O$ and $[Zn(CH_3COO)_2.2H_2O]$ in distilled water of equal volumetric concentrations. Furthermore, in this solutions the aqueous ammonia (25% NH_4OH) was mixed which formed precipitates of $Zn(OH)_2$ and $Ni(OH)_2$. Further addition of NH_4OH resulted in the dissolution of these precipitates into deep-blue colored cationic precursor solution which became the sources of Zn^{2+} and Ni^{2+} ions kept at room temperature, while hot distilled water with 1% H_2O_2 kept between 363 and 373K was used as an anionic precursor and was the source of OH^- ions . The adsorption and reaction times were optimized about 25s and 30s respectively. When the cleaned glass substrate was immersed in the cationic bath solution Zn-Ni species were adsorbed onto the surface of the substrate. The immersion of substrate in the cationic bath, rinsing with distilled water, immersion in the anionic bath and rinsing again using distilled water completes one SILAR cycle. The glass substrates were coated with the films for 20, 30 and 40 SILAR cycles. To remove excess material from the substrate following each precursor dip rinsing with distilled water is ensured so that only one ionic layer remains on the substrate before successive immersion. S1, S2 and S3 films thus deposited were annealed at 300ºC for 2hrs and S4 film were kept unannealed (Table1).

International Journal of Engineering Research & Technology (IJERT)
ISSN: 2278-0181
Vol. 13 Issue 07, July-2024

Table 1 Number of SILAR Cycles in deposition and heat treatment

Sample Name	No. SILAR Cycles	Annealed/Unannealed
S1	20	Annealed
S2	30	Annealed
S3	40	Annealed
S4	30	Unannealed

C. Characterizations

The deposited films were analyzed by different popular techniques. To identify the crystal structure PANalytical X'pert Multifunctional Powder X-ray Diffractometer (XRD) was used with Cu-Kα radiation (λ=1.54 Å). The Optical absorbance of the deposited thin films were recorded in wavelength range from 300 nm to 800 nm using Shimadzu Make UV-1800 Spectrophotometer. FTIR spectrometer: Bruker alpha model was used to record IR transmittance spectra in the range from 400 cm^{-1} to 4000 cm^{-1}.

III. RESULTS AND DISCUSSIONS

A. X-ray diffraction analysis

For unannealed samples xrd peaks represent hydroxide forms dominant as depicted in Fig.1(a) . Diffraction peaks at 2θ values marked with asterisks (*) which are indexed to $Zn(OH)_2$ phase with data from JCPDS card No. (38-0356) [16] and the peaks marked with (•) for $Ni(OH)_2$ is shown (JCDS: 14-0117)[17]. Fig. 1(b) shows the XRD patterns for samples S1, S2 and S3 annealed at 300ºC for 2 hrs. Diffraction peaks marked by point (•) for all these annealed films are indexed to the ZnO (Zinc oxide) polycrystalline hexagonal wurtzite phase, identified using JCPDS card (JCPDS: 036-1451) [18] and peaks marked by asterisk (*) indicate NiO cubic phase (JCPDS, No. 47-1049)[19]. The peaks at 31.7º, 47.7º, 57.6º and 68.3º corresponding to (100), (102), (110) and (112) respectively showed the growth of the wurtzite hexagonal phase of ZnO crystal. Cubic phase of NiO nanoparticles was identified at 64.5º corresponding to (220). XRD analysis shows that heat treatment of the films changes hydroxide form into pure oxide forms. Small shifts in XRD peaks of this nanocomposite have been observed which can be attributed to crystallographic rearrangement [7].

The average crystallite size D is calculated from the full peak width at half maximum intensity and it was estimated using Scherrer's relation [20].

$$D = 0.94\lambda/\beta\cos(\theta) \quad (1)$$

where D (in nm) is the crystallite size, λ = 1.54 Å is the wavelength of the copper k_α line , β is FWHM in radians and θ is the diffraction angle . Average crystallite sizes resulted within the range (13.1-14.1nm) as documented in Table 2 for the annealed samples S1 to S3. We observe that the average crystallite size increased (enhancement in crystallinity) with the increase in no. of SILAR cycles in deposition.

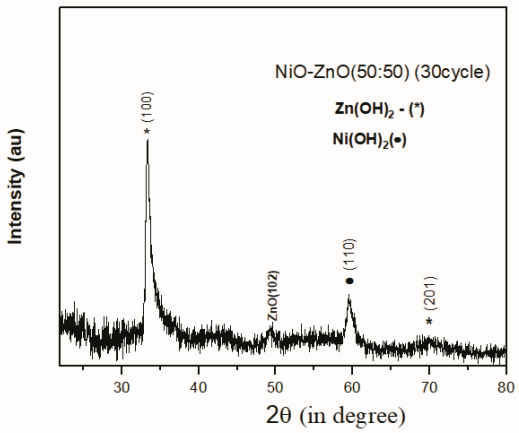

Fig.1 (a) XRD of NiO-ZnO composite unannealed film deposited for 30 SILAR cycle (S4)

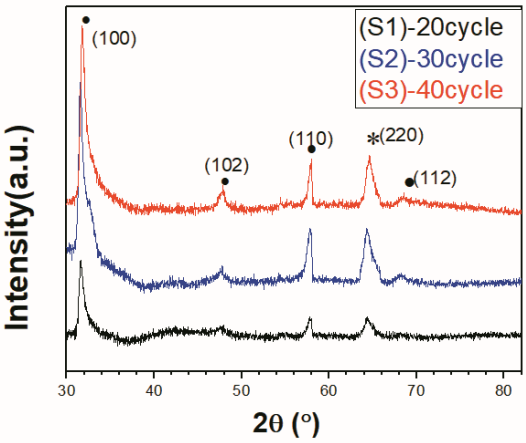

Fig.1 (b) XRD NiO-ZnO composite annealed films deposited for 20,30and 40 SILAR cycle

Published by :
http://www.ijert.org

International Journal of Engineering Research & Technology (IJERT)
ISSN: 2278-0181
Vol. 13 Issue 07, July-2024

Table 2. Average crystallite size for samples S1, S2 and S3

Sample	(hkl)	2Θ	FWHM	K	λ	D	D (avg)
Units		In degree	in degree		Å	nm	nm
S3	(100)	31.86236	0.64633	0.94	1.54178	13.36065	14.1
	(102)	47.74397	1.02059	0.94	1.54178	8.89735	
	(110)	57.83872	0.37862	0.94	1.54178	25.05601	
	(220)	64.64136	1.07894	0.94	1.54178	9.10717	
S2	(100)	31.66218	0.52843	0.94	1.54178	16.33348	13.8
	(110)	57.76159	0.54773	0.94	1.54178	17.3136	
	(220)	64.45931	1.22212	0.94	1.54178	8.03214	
S1	(100)	31.62711	0.54893	0.94	1.54178	15.72214	13.1
	(110)	57.72025	0.59325	0.94	1.54178	15.98195	
	(220)	64.44423	1.27853	0.94	1.54178	7.67712	

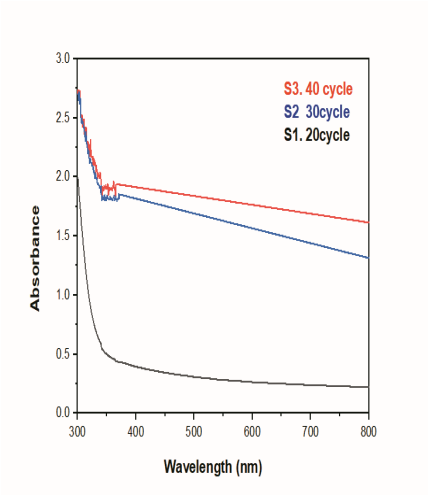

Fig.2 (b)

B. UV-Visible absorbance spectra analysis

Fig. 2(a) and (b) depicts the graph of absorbance of the films plotted against wavelength. From the graph (b) abrupt change in absorption was observed for all the films in the UV region. The absorbance increased as number of SILAR cycles increases. This increase in absorption of radiation is due to increase in film thickness as SILAR cycles increased from 20 cycles to 40 cycles. The result shows that composite thin films absorbed UV light more than visible light. Fig 2(a) shows that for unannealed film (S4) absorbance is more as compared to annealed film (S2). Also, abrupt change in absorbance is noticed at higher wavelength in annealed film.

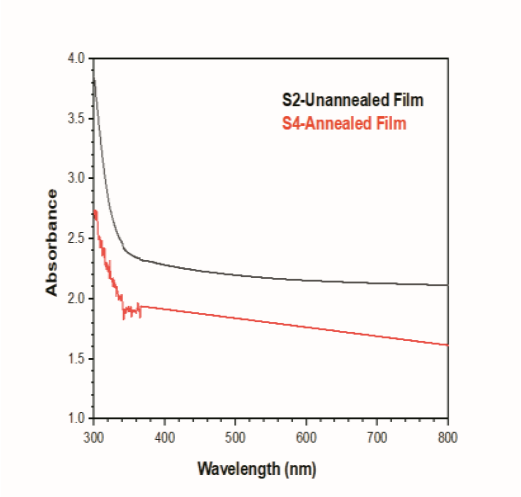

Fig.2 (a)

Fig.2 UV-Visible absorbance spectra (a) Effect of annealing on absorbance (b) Effect of SILAR cycles (20,30and 40 SILAR cycles) on absorbance

C. Film thickness measurement

The film thickness were measured by gravimetric weight method using the following equation

$$t = m/A\varrho \qquad (2)$$

where t is thickness of the film, m is mass of deposited film, A is area of the film and ϱ is the bulk density of the material. Using this equation film thickness of the samples NiO-ZnOcomposite films formed by 0.6M precursor were calculated.

D. Optical energy band gap using Tauc's plot

The absorption coefficient α can be derived from absorbance and the film thickness

$$\alpha = 2.303\ A/t \qquad (3)$$

where t is the film thickness and A is absorbance

For the direct allowed transition the absorption coefficient and optical band gap are related by the following equation

$$\alpha h\nu = B(h\nu - E_g)^{1/2} \qquad (4)$$

where B is a constant, h is the Planck constant, ν is the incident wave frequency and E_g is the energy band gap [21]. The plot between $(\alpha h\nu)^2$ and hν is shown in Fig.3 (a) and (b) for the samples. The E_g values have been deduced by extrapolating the straight line portion of the Tauc's plot at α =0 and displayed in Table 3. Single slopes indicated direct band gaps. As the number of SILAR cycle in deposition increases energy band gap is decreased (Table 3) which might be attributed to the increase in the crystallite size. Band gap decreases drastically on heat treatment as can be compared from the table 3 for samples S2 and S4.

Published by :
http://www.ijert.org

International Journal of Engineering Research & Technology (IJERT)
ISSN: 2278-0181
Vol. 13 Issue 07, July-2024

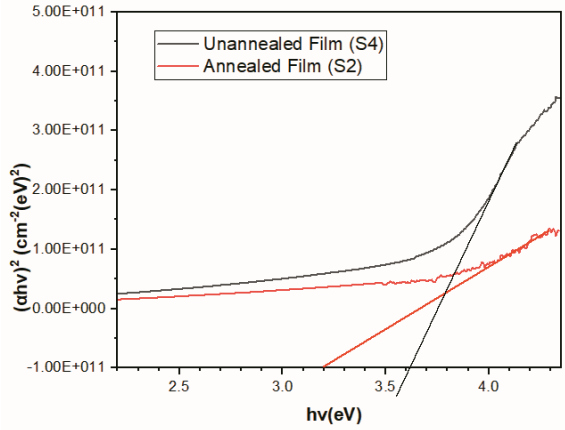

Fig.3 (a)

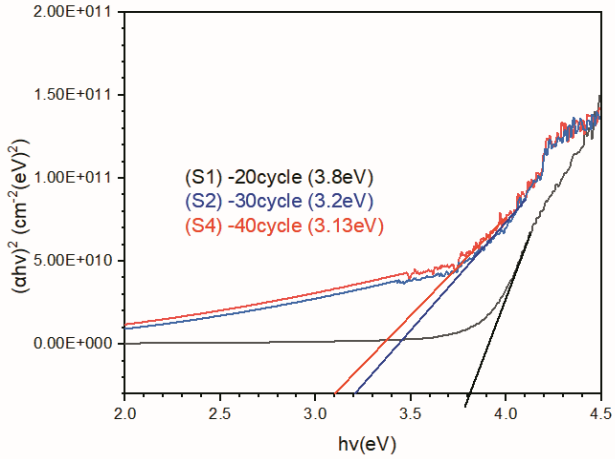

Fig. 3(b)

Fig.3 Tauc's Plots of the composite films (a) Effect of annealing on energy band gap (b)Effect of SILAR deposition cycles on energy band gap

Table 3 Optical Energy Bandgap (E_g) using Tauc's Plot

Sample Name	Obtained Value E_g(in eV)
S1(NiO-ZnO)(50:50)20Cycle	3.8
S2(NiO-ZnO)(50:50) 30Cycle	3.2
S3(NiO-ZnO)(50:50) 40Cycle	3.1
S4(NiO-ZnO)(50:50) 30Cycle (Unannealed)	3.6

E. Fourier transform infra-red (FTIR) analysis

FTIR spectra of NiO-ZnO composite films for the unannealed and annealed samples have been recorded for the range 400-4000 cm^{-1} as shown in fig 4(a) and fig.4 (b) respectively. Enlarged spectra of the same have been shown in Fig.5 (a) and 5(b) for the range from 400-700 cm^{-1} of unannealed and annealed samples respectively. In the FTIR of unannealed film band around 3500 cm^{-1} occurs due to the stretching mode of hydrogen-bonded hydroxyl groups while in the case of annealed film this is almost disappeared[22] . This is in good agreement with the XRD analysis that the annealing changes hydroxide phase into metal oxide phase. Bands at 416 $cm^{-1}$and 418 cm^{-1} are associated with the stretching of Zn–O [23]. Bands at 444 cm^{-1}, 446 cm^{-1}, 454 cm^{-1}, 471 cm^{-1}, 540 cm^{-1} and 566 cm^{-1} indicate stretching vibration of Ni-O [24]. 817 cm^{-1} represents mode bending modes O-H-O [25] 1000 to 1500 cm^{-1} is because of residual carbon species present in the precursor solution [23].

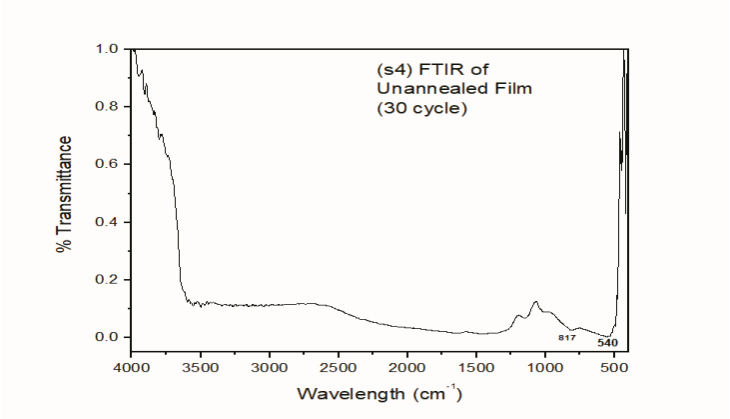

Fig.4 (a)

Published by :
http://www.ijert.org

International Journal of Engineering Research & Technology (IJERT)
ISSN: 2278-0181
Vol. 13 Issue 07, July-2024

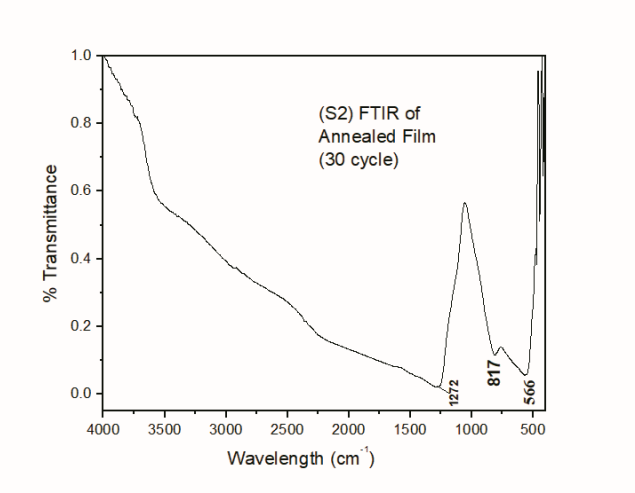

Fig.4 (b)

Fig. 4 FTIR spectra of NiO-ZnO composite film (a) Unannealed film (b) Film annealed at 300ºC for 2 hrs

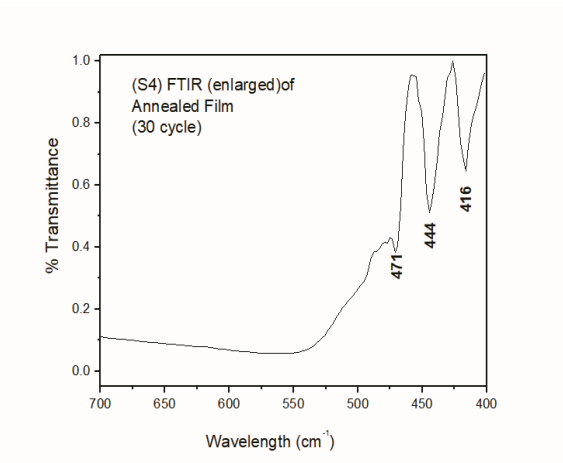

Fig.5 (b)

Fig. 5 FTIR spectra (enlarged) of NiO-ZnO composite film (a) Unannealed film (b)Annealed film at 300ºC for 2 hrs

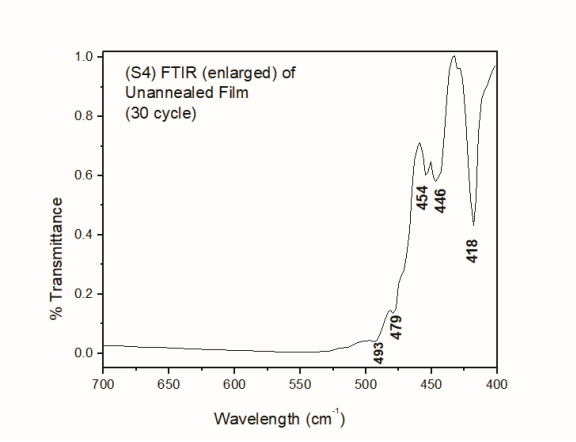

Fig.5 (a)

International Journal of Engineering Research & Technology (IJERT)
ISSN: 2278-0181
Vol. 13 Issue 07, July-2024

IV. CONCLUSION

NiO-ZnO nanocrystalline thin films were deposited on glass substrate via SILAR method using cationic precursor which contained equal mixing percentages of cationic solution for NiO and ZnO at 0.6M for 20, 30 and 40cycles . The deposited thin films both unannealed and annealed at 300ºC for 2 hrs were subjected to optical and structural characterization. The XRD results showed dominant hydroxide phase for unannealed sample and annealed ones showed peaks for oxide phases and no appearance of secondary phases. The crystallite size exhibited an enhancement of the crystallinity (13.1-14.1nm) as the no. of SILAR cycle increased (20-40 cycles). Absorbance results showed that the absorbance of the films increased as number of SILAR cycles increased and decreased as wavelength increased. Optical energy band gap of the films calculated using Tauc's plot fell between 3.1eV and 3.8eV. The energy band gap was found to decrease as number of SILAR cycle increases. This decrease in band gap is as a result of increase in the crystallite size. Comparison of optical properties of annealed and unannealed films revealed that heat treatment of films decreases optical band gap significantly .The Energy band gap of the NiO-ZnO nanocomposite films can be customized as required for particular application by varying no. of SILAR cycles. FTIR results confirmed the XRD analysis that heat treatment of the films changes the hydroxide phase into nanocomposite metal oxide phase.

REFERENCES

[1] N.P. Klochko, V.R. Kopach, I.I. Tyukhov, D.O. Zhadan, K.S. Klepikova, G.S. Khrypunov, S.I. Petrushenko, V.M. Lyubov, M.V. Kirichenko, S.V. Dukarov and A.L.. Khrypunova, " Metal oxide heterojunction (NiO/ZnO) prepared by low temperature solution growth for UV-photodetector and semi-transparent solar cell ," Solar Energy, vol. 164, pp.149-159, 2018.

[2] A.C. Nwanya, P.R. Deshmukh, R. U. Osuji de, M. Maaza, C.D. Lokhande and F. L. Ezemade "Synthesis, characterization and gas-sensing properties of SILAR deposited ZnO-CdO nano-composite thin film ," Sensors and Actuators B: Chemical , vol. 206, pp. 671-678, 2015.

[3] S.N. Pusawale and P.S. Jadhavab, "Effect of surface treatments on supercapacitive perfor of sno2-ruo2 composite thin films," Materials Today: Proceedings , vol. 18 pp. 2848–2858 , 2019.

[4] W. J. Huang, S. A. De Valle, J. B. Kana Kana, K. Simmons-Potter and B. G. Potter, "Integration of CdTe-ZnO nanocomposite thin films into photovoltaic devices," Sol. Energy Mater. Sol. Cells, vol. 13, pp. 86–92, 2015.

[5] S. Noothongkaew , O. Thumthan and Ki-Seok An , "UV-Photodetectors based on CuO/ZnO nanocomposites ," Material letters , vol. 233, pp.318-323, 2018.

[6] G. Vijayaprasath, P. Sakthivel, R. Murugan, T. Mahalingam, and G. Ravi, "Deposition and characterization of ZnO/NiO thin films," in AIP Conference Proceedings, 1731, 080033 2016. [American Institute of Physics Inc.]

[7] S. Thamri, I. Sta, M. Jlassi, M. Hajji, and H. Ezzaouia, "Fabrication of ZnO-NiO nanocomposite thin films and experimental study of the effect of the NiO, ZnO concentration on its physical properties," Mater. Sci. Semicond. Process. vol. 71, pp. 310–320, Nov. 2017.

[8] A. I. Inamdar, Y. Kim, S. M. Pawar, J. H. Kim, H. Im, and H. Kim, "Chemically grown, porous, nickel oxide thin-film for electrochemical supercapacitors," J. Power Sources, vol. 196, pp. 2393–2397, Feb. 2011.

[9] J. Huang , B. Li , Y. Hu , X. Zhou , Z. Zhang , Y. Ma , K.Tang , L.Wang and Y. Lu., "Transparent p-NiO/n-ZnO heterojunction ultraviolet photodetectors prepared on flexible substrates," Surf. Coatings Technol., vol. 362, pp. 57–61, Mar. 2019.

[10] R. S. Kate, S. A. Khalate, and R. J. Deokate, "Electrochemical properties of spray deposited nickel oxide (NiO) thin films for energy storage systems," J. Anal. Appl. Pyrolysis, vol. 125, pp. 289–295, May 2017.

[11] B. C. Ghos, S. F. U. Farhad, Md. A. M. Patwary, S. Majumder, Md. A.Hossain, N.I.Tanvir, M. A. Rahman, T. Tanaka and Q. Guo "Influence of the substrate, process conditions, and postannealing temperature on the properties of zno thin films grown by the successive ionic layer adsorption and reaction method" ACS Omega, Vol.6, pp.2665-2674 , 2021.

[12] X. Liu, J. Zhang, X. Guo, S.Wu and S. Wang, "Amino acid-assisted one-pot assembly of Au, Pt nanoparticles onto one-dimensional ZnO microrods," Nanoscale, vol. 2, pp.1178–1184, 2010.

[13] A. M. Reddy, A. S. Reddy, K. S. Lee and P. S. Reddy, "Growth and characterization of NiO thin films prepared by dc reactive magnetron sputtering," Solid State Sci., vol. 13, pp. 314–320, Feb. 2011.

[14] Q. A. Adeniji, K. Odunaike, T. O. Fowodu, and A. T. Talabi, "Influence of silar cycle on the energy bandgap of iron copper sulphide (FeCuS) thin films deposited on SLG substrate," NanoWorld J., vol. 5, pp. 49–52, 2019.

[15] P. Sreedev ,V.Rakhesh , N.S.Roshima and S. Balakrishnan , "Preparation of zinc oxide thin films by SILAR method and its optical analysis," Journal of Physics: Conf. Series 1172 , 012024, 2019.

[16] F. V. Molefe , L. F. Koao, B. F. Dejene and H. C. Swart, "Phase formation of hexagonal wurtzite ZnO through decomposition of $Zn(OH)_2$ at various growth temperatures using CBD method," Optical Materials , vol.46, pp.292-298,2015.

[17] Y.Qu, W. Zhou, X.Miao, Y. Li , L. Jiang, K. Pan, G. Tian, Z. Ren, G. Wang and H. Fu, "A new layered photocathode with porous nio nanosheets: An effective candidate for p-type dye-sensitized solar cells," Chem. Asian J. , Vol. 8, pp. 3085 – 3090, 2013.

[18] D. Paul, S. Maiti, D. P. Sethi, and S. Neogi, "Bi-functional NiO-ZnO nanocomposite: Synthesis, characterization, antibacterial and photo assisted degradation study," Adv. Powder Technol. Vol.32, pp.131, 2021.

[19] M. R. Das, A. Roy, S. Mpelane, A. Mukherjee, P. Mitra, and S. Das, "Influence of dipping cycle on SILAR synthesized NiO thin film for improved electrochemical performance," Electrochim. Acta, vol. 273, pp. 105–114, May 2018.

[20] N. S. Al-Din, A. Khoudro and M. Mohamad, "Structural and optical properties of zno-nio nanocomposite thin films deposited by spray pyrolysis," IJERT, vol. 10, oct.2021.

[21] A. Santhamoorthy, P.Srinivasan, A. Krishnakumar, J. B. B. Rayappan and K J. Babu , "SILAR-deposited nanostructured ZnO thin films: effect of deposition cycles on surface properties," Bull. Mater. Sci., vol. 44 , pp. 188, 2021.

[22] N. Rauf , S. Ilyas , H. Heryanto , R. Rahmat , A. N. Fahri , M. H.Rahmi , D. Tahir , "The correlation between structural and optical properties of zinc hydroxide nanoparticle in supports photocatalytic performance " Optical Materials, vol.112, pp. 110780, 2021.

[23] A. K. Zak, W. H. A. Majid, M. Darroudi, and R. Yousefi, "Synthesis and characterization of ZnO nanoparticles prepared in gelatin media," Mater. Lett., vol. 65, pp. 70–73, Jan. 2011.

[24] R. Barir, B. Benhaou, S. Benhamid, A. Rahal, T. Sahraoui and R. Gheriani, "Effect of precursor concentration on structural optical and electrical properties of nio thin films prepared by spray pyrolysis," J. Nanomater., vol. 2017, 2017.

[25] A. J. Haider, R. Al-Anbari, H. M. Sami, Md. J. Haider, "Enhance preparation and characterization of nickel-oxide as self- cleaning surfaces" Energy Procedia , vol. 157, pp.1328-1342 , 2019.